Supporting Information

Tailoring the Optical Response of Pentacene Thin Films via Templated Growth on Hexagonal Boron Nitride

Samuel H. Amsterdam,[1,†] Trevor LaMountain,[2,†] Teodor K. Stanev,[3,†] Vinod K. Sangwan,[4] Rafael López-Arteaga,[1] Suyog Padgaonkar,[1] Kenji Watanabe,[5] Takashi Taniguchi,[6] Emily A. Weiss,[1,2,4] Tobin J. Marks,[1,4] Mark C. Hersam,[1,2,4,7*] and Nathaniel P. Stern[2,3*]*

[1] Department of Chemistry and the Materials Research Center, Northwestern University, Evanston, Illinois 60208, USA

[2] Applied Physics Program, Northwestern University, Evanston, Illinois 60208, USA

[3] Department of Physics and Astronomy, Northwestern University, Evanston, Illinois 60208, USA

[4]Department of Materials Science and Engineering and the Materials Research Center, Northwestern University, Evanston, Illinois 60208, USA

[5]Research Center for Functional Materials, National Institute for Materials Science, 1-1 Namiki, Tsukuba 305-0044, Japan

[6]International Center for Materials Nanoarchitectonics, National Institute for Materials Science, 1-1 Namiki, Tsukuba 305-0044, Japan

[7]Department of Electrical Engineering and Computer Science and the Materials Research Center, Northwestern University, Evanston, Illinois 60208, USA

[†]These authors contributed equally

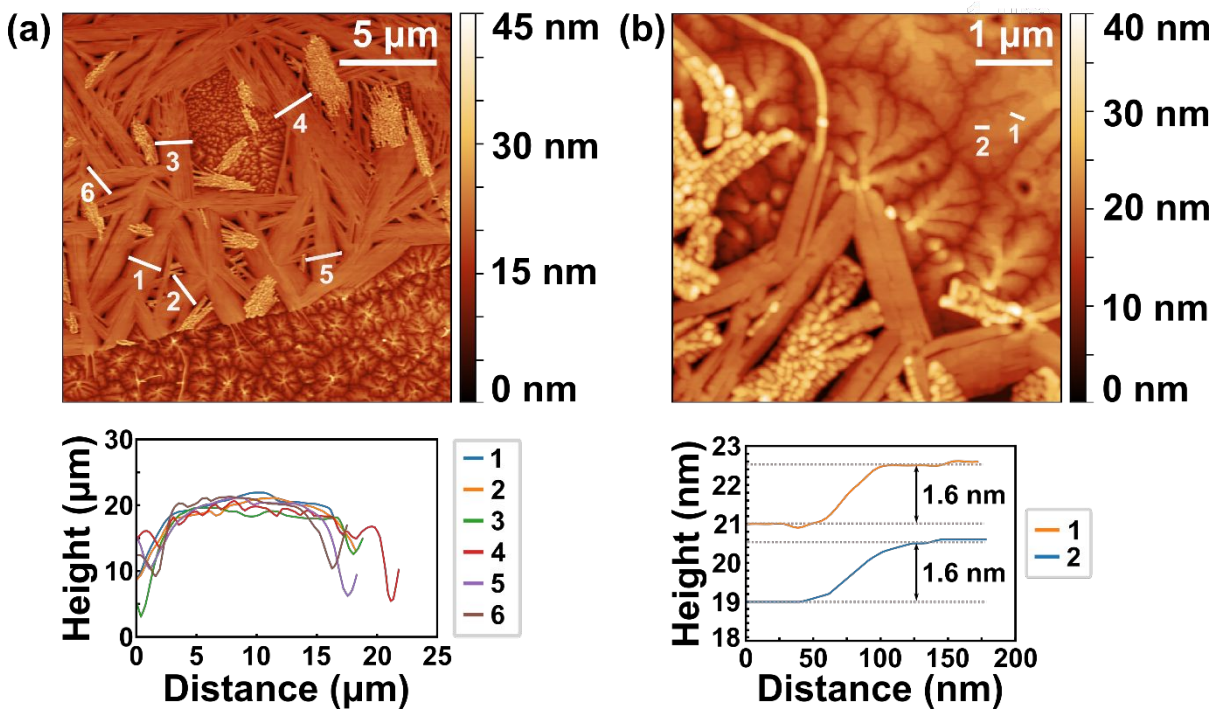

Figure S1. (a) AFM profilometry of large pentacene needles on hBN showing heights of 10 – 20 nm and widths of 1 – 2 μm. (b) AFM profilometry of pentacene terraces on SiO_2. The step height is 1.6 nm, consistent with the thin-film phase.

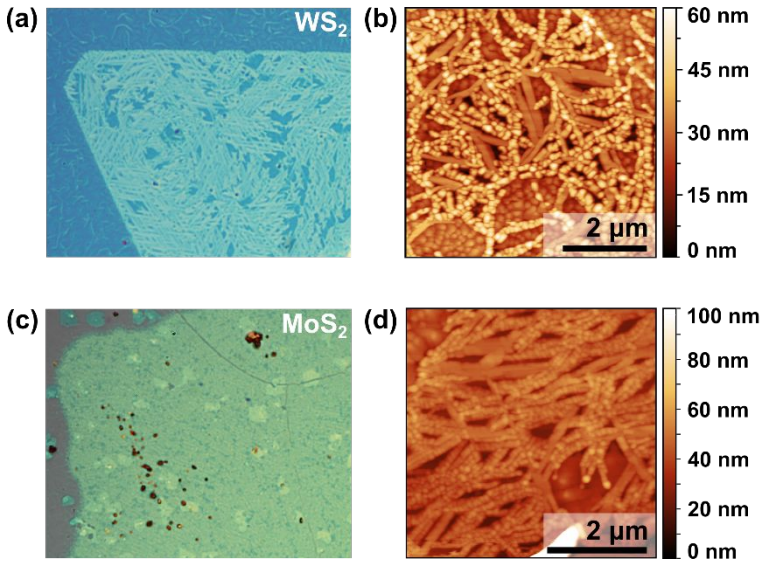

Figure S2. π-Face-on and thin-film phase of pentacene on semiconducting vdW materials. (a,c) Optical images at 100x magnification of pentacene on WS_2 (a) and MoS_2 (c). (b, d) AFM scans of (a, c) respectively. Needle-like structures are apparent on both. They also show a greater coverage of nanoscale grains and dendritic thin-film phase than on hBN.

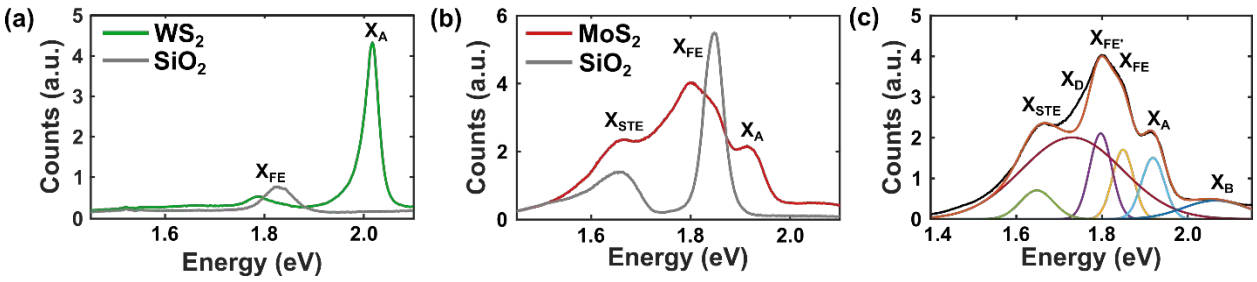

Figure S3. (a,b) PL spectra at 10 K of pentacene thin films on the indicated vdW substrates compared to SiO_2. Red-shift of the pentacene peak on WS_2 is apparent since the WS_2 exciton is well-separated from the pentacene emission. The pentacene/MoS_2 spectrum is more complicated since the pentacene emission overlaps spectrally with the MoS_2 emission. X_A denotes the A-exciton emission of the vdW material, X_{FE} denotes the pentacene free exciton emission, and X_{STE} denotes the pentacene self-trapped exciton. The STE emission of pentacene on WS_2 is hidden by the large intensity of the A-exciton

emission. (c) The pentacene/MoS_2 spectrum broken down by a series of peak functions in order to better identify the constituent components of the broad, convoluted emission. In addition to the peaks in (b), there is contribution from the MoS_2 B-exciton (X_B), the MoS_2 defect emission (X_D), and both the thin-film and π-face-on phase pentacene FE emission (X_{FE} and $X_{FE'}$ respectively)

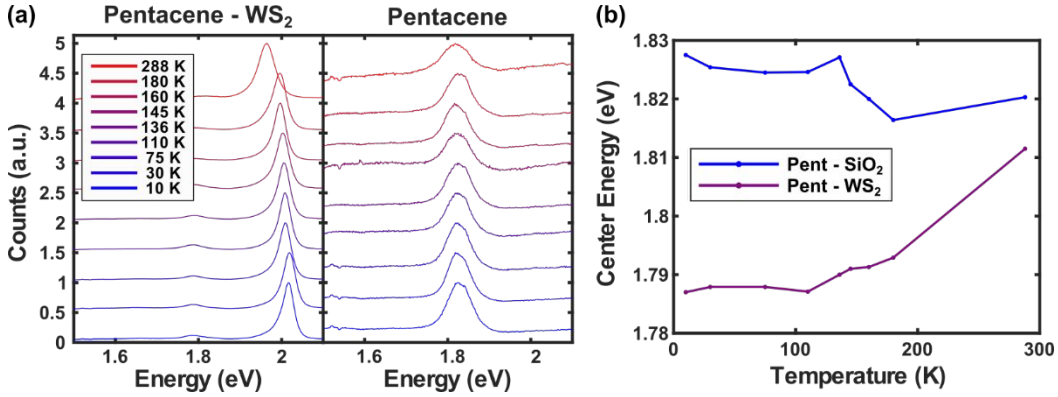

Figure S4. Temperature-dependent PL of pentacene/WS_2. (a) PL plots of the pentacene thin films on WS_2 and SiO_2. The WS_2 exciton emission at 2 eV is more efficient than the pentacene free exciton at 1.8 eV. (b) Energy of pentacene free exciton emission versus temperature. The epitaxial film on WS_2 behaves similarly to the film on hBN, although with a lower overall energy shift.

The in-plane thermal expansion coefficient of WS_2 is on the order of 10^{-6} K^{-1}, based on temperature-dependent Raman measurements.[1] This thermal expansion coefficient is between hBN (2 - 4 × 10^{-5} K^{-1})[2] and SiO_2 (5 × 10^{-7} K^{-1}),[3] which aligns with the temperature-dependent PL shift of pentacene/WS_2 being between those two other substrates.

Table S1. Fitting parameters for the photoluminescence decay histograms of pentacene deposited on an hBN flake and on a non-hBN part of the substrate, excited at 570 nm. Three spots were evaluated at each region on the image. The IRF was fitted to a Gaussian (a_1, τ_1) and a biexponential decay (a_2, τ_2, a_3, τ_3).

Spot	a_1 [%]	τ_1 [ps]	a_2 [%]	τ_2 [ns]	a_3 [%]	τ_3 [ns]	$<\tau>$ [ps]
Off 1	> 99.99	< 50	< 0.01	0.40±0.02	---	---	< 50
Off 2	> 99.99	< 50	< 0.01	0.40±0.03	---	---	< 50
Off 3	> 99.99	< 50	< 0.01	0.39±0.02	---	---	< 50
On 1	> 99.99	< 50	< 0.01	0.40±0.02	< 0.01	3.20±0.28	< 50
On 2	> 99.99	< 50	< 0.01	0.40±0.02	< 0.01	3.10±0.24	< 50
On 3	> 99.99	< 50	< 0.01	0.40±0.02	< 0.01	3.10±0.19	< 50
Wrinkle 1	> 99.99	< 50	< 0.01	1.20±0.11	< 0.01	4.20±0.18	60±10
Wrinkle 2	99.97±0.01	< 50	0.03±0.02	0.85±0.03	< 0.01	3.40±0.14	200±10
Wrinkle 3	> 99.99	< 50	< 0.01	1.10±0.14	< 0.01	4.10±0.17	< 50
IRF	(Gaussian)	29±1	95.6±0.3	0.011±0.001	4.4±0.1	0.219±0.001	

REFERENCES

(1) Huang, X.; Gao, Y.; Yang, T.; Ren, W.; Cheng, H. M.; Lai, T. Quantitative Analysis of Temperature Dependence of Raman Shift of Monolayer WS_2. *Sci. Rep.* **2016**, *6* (1), 1–8. https://doi.org/10.1038/srep32236.

(2) Yates, B.; Overy, M. J.; Pirgon, O. The Anisotropic Thermal Expansion of Boron Nitride: I. Experimental Results and Their Analysis. *Philos. Mag.* **1975**, *32* (4), 847–857. https://doi.org/10.1080/14786437508221624.

(3) Blech, I.; Cohen, U. Effects of Humidity on Stress in Thin Silicon Dioxide Films. *J. Appl. Phys.* **1982**, *53* (6), 4202–4207. https://doi.org/10.1063/1.331244.